CRC #74: Mitigation of steel reinforcement corrosion via bioactive agents: Final Report

Aaron R. Sakulich[1] and Jessica D. Schiffman[2]
[1]Department of Civil and Environmental Engineering, Worcester Polytechnic Institute, Worcester, MA, 01609
[2]Department of Chemical Engineering, University of Massachusetts Amherst, Amherst, MA, 01003

Problem Statement:

The corrosion of reinforcing steel in concrete can reduce the service life of a structure [1, 2]. This phenomenon is commonly initiated when a structure is exposed to aggressive media (e.g. deicing salts or seawater) which depassivates the steel and leads to the formation of rust [3]. Since rust expands during creation, pressure is generated that leads to cracking and spalling [4, 5]. Cracks are particularly undesirable because they allow easier access for aggressive media to travel through the cementitious matrix, accelerating deterioration [6, 7]. Although many corrosion mitigation methods are on the market today, $100 billion is still being expended worldwide each year on corrosion related damage [8]. New corrosion mitigation methods are needed.

Earlier research has demonstrated that bioactive agents such as cinnamaldehyde mitigate corrosion but, when incorporated in a cementitious matrix, negatively affect the hydration of cement and lower compressive strength [9]. A novel delivery method that avoids this issue is encapsulation in lightweight aggregate (LWA). LWA has been previously used in a method known as internal curing (where LWA is pre-soaked with water) to prevent early age cracking and enhance durability. When added to concrete along with other aggregates, the LWA releases liquid in its pores as the cement hydrates, which can then migrate towards the reinforcing steel to create a protective barrier. In this way the properties of the concrete will not be disturbed [10].

Project Objectives:

This experimental study aimed to investigate an innovative cinnamaldehyde-LWA inhibitor that can be added to a cementitious mix in order to protect reinforcing steel from corrosion. By protecting the reinforcing steel, the service life of structures can be extended and the billions of dollars lost annually due to corrosion will not have to be expended. Several tests and studies were carried out in order to better understand the use of cinnamaldehyde-LWA inhibitor in a cementitious matrix. Therefore, this experimental program was separated into two phases: Phase I and Phase II.

> *Phase I* was a preliminary study where the chemical and mechanical properties of a cementitious mix incorporating cinnamaldehyde-LWA inhibitor were investigated. Moreover, the cementitious mix was examined when exposed to a corrosive environment. This study was also compared to a commercially available surface-applied penetrating corrosion inhibitor. The surface-applied penetrating corrosion inhibitor was similarly encapsulated by LWA. Since penetrating corrosion inhibitor is applied to the surface of a structure, the time for it to reach and protect the rebar may be shortened if the inhibitor is encapsulated in the LWA.
>
> *Phase II* was a continuation of Phase I. It focused on the impact of transport properties (e.g. sorptivity and diffusion) within the cementitious mix and the effect on rebar pullout when incorporating cinnamaldehyde-LWA inhibitor.

During this experimental program, one PhD candidate, three high school students and one undergraduate student from a NSF funded program - Research Experience for Undergraduates (REU) – worked on this project. Two journal papers have been submitted as a result of this study. Two conferences proceedings were also published:

Jafferji, H.K., Gregory T.; Schiffman, Jessica D.; Sakulich, Aaron R., *Preliminary Investigations of Essential Oils as Corrosion Inhibitors in Steel Reinforced Cementitious Systems.* Proceeding of the Thrity-Fifth Conference on Cement Microscopy, USA, 2013: p. 40-48.

Jafferji, H. and A.R. Sakulich. *Impact of Corrosion Inhibitors on Design*. Proceedings of the 2nd International Workshop on Design in Civil and Environmental Engineering, Worcester, MA, USA. 2013.

Phase I:

This preliminary investigation consisted of eight tests: air content, setting time, compressive strength, semi-adiabatic calorimetry, autogenous shrinkage, accelerated corrosion test (ACT), electrical resistivity, and steel mass loss. The next sections describe the materials and methods used in this experimental study followed by the results and discussion.

Materials and Methods

All mixes were prepared with commercially available ASTM C150 Type I/II cement. Local sand was used throughout and the particle size distribution was determined by sieve analysis. Sand retained on sieve sizes 8, 16, 30, 50, and 100 were included in all mix designs. The three liquids that were soaked and encapsulated within the LWA were: cinnamaldehyde (C_9H_8O), a commercially available penetrating corrosion inhibitor, and water. Expanded shale LWA (Northeast Solite Corporation) was used to encapsulate the internal agents. In order to reduce the amount of cinnamaldehyde entering a mix, fine LWA particles (which retain cinnamaldehyde on the surface because of its high surface area) were removed and only LWA retained on a No. 8 or No. 16 sieve were used in the production of samples.

To encapsulate the liquids into the LWA, LWA was soaked at room temperature in the appropriate liquids for at least 24 h in an airtight container. These LWA-soaked liquids were incorporated into the mix at a saturated-surface-dry (SSD) state. A water:cement (w/c) ratio of 0.4 (not including any water added via LWA, if applicable) and a 55 % volume fraction of aggregate were used in all mix designs. Aggregates were either sand or a mix of LWA and sand. LWA replaced sand on a volumetric basis in order to ensure a constant particle size distribution and accurate comparison between mixtures.

A total of six mortar mixes were produced (Table 1). Mix 1 was a control where only sand, cement and water were used. Mix 2 included cinnamaldehyde-LWA inhibitor; Mix 3 was the same as Mix 2, but included water instead of cinnamaldehyde. Mix 4 contained penetrating corrosion inhibitor-LWA; Mix 5 was the same as Mix 4, but with water in place of the penetrating corrosion inhibitor. In this way, Mixes 1, 3, and 5 served as controls enabling the identification of changes in physicochemical properties due to the incorporation of LWA (as opposed to due to the cinnamaldehyde and penetrating corrosion inhibitor). In a final mix, Mix 6, penetrating corrosion inhibitor was applied to the surface in three 24 h intervals 24 h after demolding. For comparison purposes, only Mix 6 underwent the accelerated corrosion test and was evaluated for electrical resistivity and mass steel loss.

Table 1: Mix designs for mortars in used in Phase I: The total sum of the aggregate for each design is 1375 cm3 (1 in3 = 16.4 cm3). In order to prevent cinnamaldehyde and penetrating corrosion inhibitor from remaining on the surface of the LWA, larger LWA particle sizes (retained on #8 and #16 sieves) were used. Mix 6 followed the same distribution as Mix 1 but had penetrating corrosion inhibitor sprayed on the surface.

Mixture	Mix 1 (cm^3)	Mix 2 (cm^3)	Mix 3 (cm^3)	Mix 4 (cm^3)	Mix 5 (cm^3)	Mix 6 (cm^3)
Cement	464.6	464.6	464.6	464.6	464.6	464.6
Water	585.4	585.4	585.4	585.4	585.4	585.4
Aggregate						
#8 Sand	200.8	82.7	82.7	72.6	72.6	200.8
#16 Sand	220.0	90.7	90.7	79.6	79.6	220.0
#30 Sand	360.3	360.3	360.3	360.3	360.3	360.3
#50 Sand	468.9	468.9	468.9	468.9	468.9	468.9
#100 Sand	125.1	125.0	125.0	125.1	125.1	125.1
#8 LWA	-	118.0	118.0	128.1	128.1	-
#16 LWA	-	129.4	129.4	140.4	140.4	-
CA	-	75	-	-	-	-
PCI	-	-	-	75	-	-
Internal Water	-	-	75	-	75	-

X-ray diffraction (XRD) and Fourier transform infrared spectroscopy (FTIR) were conducted on the as-received ordinary portland cement (OPC) for quality control purposes (Fig. 1). Alite (C_3S), belite (C_2S), and celite (C_3A) were detected by XRD. Five bands were identified with FTIR. Bands at 601.8 cm^{-1} and 663.5 cm^{-1} were due to Si-O vibrations; the band 881.5 cm^{-1} was due Si-O, Al-O, CO_3^{2-} vibrations; the band at 1153.4 cm^{-1} was due to S-O vibrations; and the band at 1438.9 cm^{-1} was due to CO_3^{2-}. These results are consistent with standard ready-mix ordinary portland cement.

Compressive strength tests were performed according to ASTM C109. Mortar was placed in 2 in. (50 mm) cube molds, which were then placed in a plastic bag, stored in a fog room, and demolded after 24 h. The cubes were stored uncovered at 70 °F and 99 % humidity during curing. Three mortar cubes from each mix design were tested at ages of 3, 7, and 28 d. Setting time was determined in accordance with ASTM C191 and the air content of the mortar was measured in accordance with ASTM C185. Air contents were measured to be 3.8 % (Mix 1), 2.2 % (Mix 2), 3.5 % (Mix 3), 4.4 % (Mix 4), and 3.1 % (Mix 5). This suggests that the air content is not significantly impacted by the internal agents, and was not further investigated.

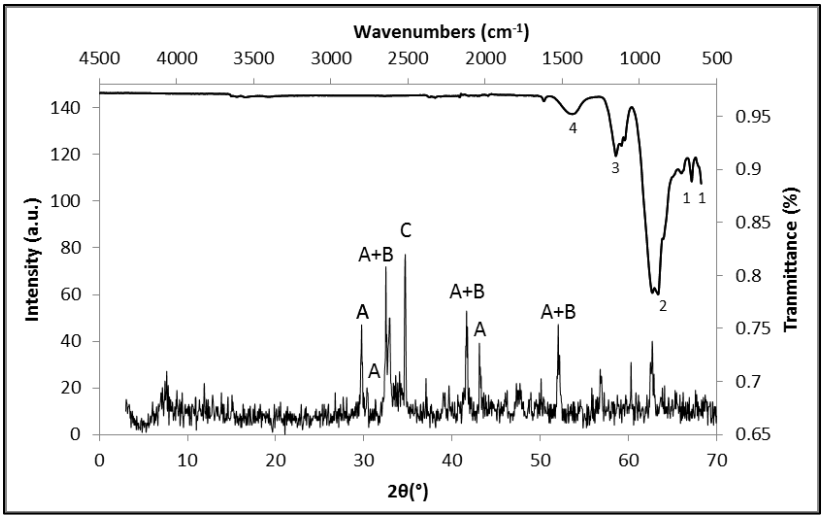

Figure 1: XRD (primary axes) and FTIR spectra (secondary axes) of the OPC. A = alite; B = belite; C = celite. Bands at 1 = 601.8 cm^{-1} and 663.5 cm^{-1} were due to Si-O vibrations; the band 2 = 881.5 cm^{-1} was due Si-O, Al-O, CO_3^{2-} vibrations; the band at 3 = 1153.4 cm^{-1} was due to S-O vibrations; and the band at 4 = 1438.9 cm^{-1} was due to CO_3^{2-}.

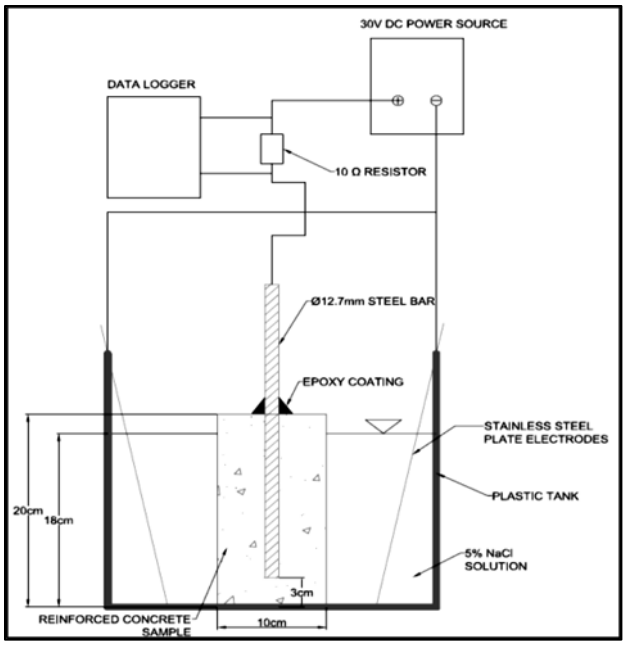

Figure 2: Schematic of accelerated corrosion test (ACT).

Semi-adiabatic calorimetry was used to characterize potential interference in hydration reactions due to the additional liquids (cinnamaldehyde, penetrating corrosion inhibitor, and water), which would appear as an alteration of heat evolution during the exothermic cement hydration processes. Specimens were cast in 4 x 8 in. (100 x 200 mm) cylinder molds with type K thermocouples embedded in the center. The entire cylinder was insulated and the rise in sample temperature recorded for 3 d.

Autogenous shrinkage was measured according to ASTM C1698 as an indirect way of determining whether internal agents are diffusing out of the LWA – a reduction of autogenous shrinkage may indicate that the internal agents are entering the pore system, reducing the surface tension of pore solution. Between measurements, specimens (at least three per mix design) were stored in two layers of plastic bags and placed in 70 °F and 99 % humidity to ensure constant curing conditions.

Accelerated corrosion tests (ACT) were conducted on experimental samples based on designs found in the literature [11, 12]. Three samples were investigated per mix design. Mortar was placed into a 4 x 8 in. (100 x 200 mm) cylinder, and a jig was used to hold a 0.5 in. (12.7 mm) piece of wire-brushed steel rebar in the center (Fig. 2). Due to this shape, the samples are generally referred to as "lollipop" specimens [13, 14]. Epoxy coating was used around the top of the rebar to prevent crevice corrosion. The lollipop samples were placed in a plastic tank containing 5 wt.% NaCl solution after 28 days of curing; two stainless steel plates were placed near the sample; and a 30 V DC power source was used to accelerate the corrosion. A data logger recorded current through the rebar, with a rapid increase in current signifying cracking. In addition to the current readings, the electrical resistivity of each sample was quantified using the Wenner technique [15]. Four readings were taken for each of the lollipop samples from the beginning of the ACT until cracking failure of the sample. The current was recorded until complete failure of the lollipop sample; complete failure was determined by visual inspection and defined as severe cracking in the sample (Fig. 3). Similar trends have been observed in various other studies which have conducted accelerated corrosion tests [11, 14, 16-18]. Finally, the mass loss of the reinforcing steel over the course of the ACT was calculated using Faraday's law:

$$M = \frac{A_w \cdot \int I dt}{n \cdot F} \qquad (1)$$

where, M is the mass loss (g); A_w is the atomic weight of iron (55.86 g/mole); $\int Idt$ is the current x time relation (A•sec); n is

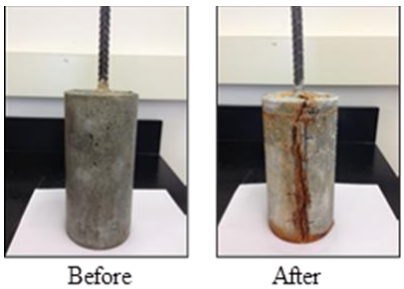

Figure 3: Lollipop sample prior to ACT (left); failure of sample after undergoing ACT (right).

the ferrous valency (2); F is Faraday's constant (96,485.3 coulombs/mole of ferrous).

Table 2: Initial and final setting times for each mix

Mixture	Initial Setting Time (min)	Final Setting Time (min)
Mix 1	75	150
Mix 2	75	195
Mix 3	165	240
Mix 4	165	345
Mix 5	120	210

Experimental results and discussion

The addition of internal agents increased the set times of all mixes (Table 2). Although Mix 2 produced the same initial set time as Mix 1, its final set time was prolonged by 45 min. The initial set of both Mixes 3 and 4 were prolonged by 90 min (55 %); that of Mix 5 was prolonged by 45 min (38 %). Final setting times for Mixes 3, 4, and 5 increased by 90 min (38 %), 195 min (57 %), and 60 min (29 %), respectively. The lengthened setting times of Mixes 2 and 4 is likely due to the cinnamaldehyde and penetrating corrosion inhibitor remaining on the surface of the LWA after pre-soaking. This material then enters the mix water and hinders the reaction between cement particles and water. In Mixes 3 and 5, the water remaining on the surface of the LWA causes a slight increase to the initial w/c ratio, which may prolong the setting time.

Mixes that did not incorporate cinnamaldehyde or penetrating corrosion inhibitor had similar strength profiles (Fig. 4). Mix 3 and Mix 5 achieved comparable but slightly lower strengths than Mix 1. Bentz observed similar behavior of a slight reduction in compressive strength and determined it to be a result to the relatively weak porous LWA [19]. The strengths of Mix 2 did not greatly increase with time; the 3 d strength did not significantly increase on day 7 and 28. The same trend was observed with Mix 4. Although some of the decreases in the strengths of both Mixes 2 and 4 are due to the LWA, which is mechanically weak, further reductions in compressive strength are likely due to either the cinnamaldehyde and the penetrating corrosion inhibitor diffusing out of the LWA and interfering with the hydration reactions, or surplus liquid remaining on the surface of the LWA, entering the mix water, and causing interference.

Hydration is an exothermic reaction; as such, an alteration of the temperature profile of a cementitious system under otherwise identical curing conditions indicates interference with hydration. The heat evolution of Mixes 2, 3, 4, and 5 were decreased compared to the control (Fig. 5). Mixes 2 and 4 experienced a 6 % and 3 % reduction in peak temperature compared with the peak temperature of 61.5° in Mix 1, respectively. A slightly different trend was observed for Mixes 3 and 5. The rate of hydration was accelerated, producing a leftward shift in the graph with an overall lower peak temperature (8.5 % and 10.8 % decreases, respectively).

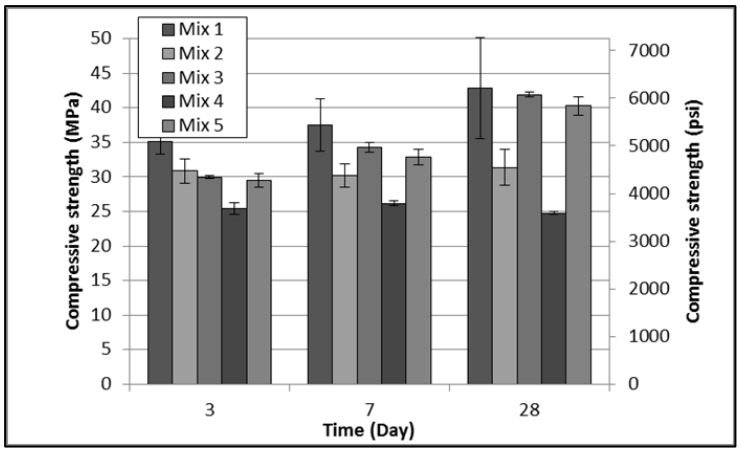

Figure 4: Compressive strength of mortars at days 3, 7, and 28 as tested by ASTM C109

As with the set time and compressive strength, the semi-adiabatic calorimetry results indicate an interference with the

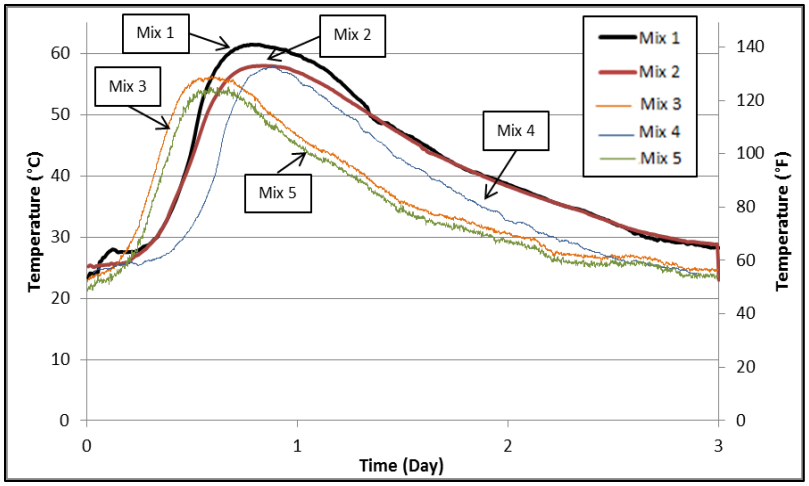

Figure 5: Semi-adiabatic calorimetry

hydration reactions. However, the situation is complicated by the fact that water encapsulated in the LWA has a higher heat capacity than quartz or the other internal agents and therefore takes longer to increase in temperature. During a similar experiment, Bentz *et al.* observed similar accelerations as observed here for Mixes 3 and 5 [20]. The peak temperatures observed by Bentz *et al.* exceeded those observed here, likely due differences in sample size between the two experiments.

Mix 1 experienced autogenous shrinkage, while Mixes 2, 3, 4, and 5 were shown to expand (Fig. 6). Bentur *et al.* performed similar autogenous shrinkage tests on samples containing water-LWA and also observed expansion, apparently due to continued hydration spurred by the additional supply of water released from the LWA and the prolonged saturation of pores [21]. The expansion observed in Mix 2 (containing the cinnamaldehyde-LWA) and Mix 4 (containing the penetrating corrosion inhibitor-LWA), suggests that the internal agents are diffusing from the LWA into the pores of the cementitious matrix, more completely saturating pores and reducing the surface tension of pore solution (and thus reducing shrinkage).

In the ACT, a certain current flowing through the sample is required in order to keep the anodic potential constant (Fig. 7). Currents in Mixes 1, 3, 4, 5, and 6 followed a similar trend: the current begins at a range between 0.22 A and 0.26 A and gradually decreased with time. Eventually, a sharp and significant increase in current occurred, indicating the initiation of a crack and direct exposure of the rebar to the chloride solution. Mix 2 experienced the same trend but at a current of roughly 0.05 A. This may be due to the fact that cinnamaldehyde is an organic material. Organic materials are known to have a relatively high electrical resistivity, which would serve to reduce the current [22].

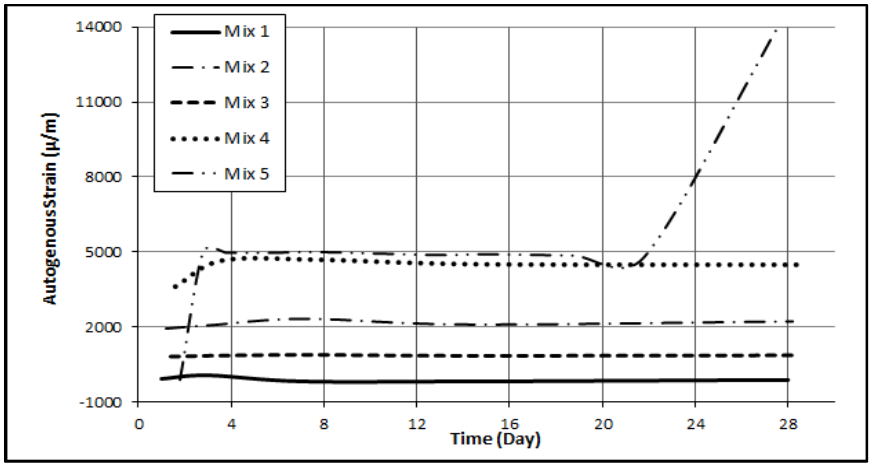

Figure 6: Autogenous strain

The average cracking time for five of the six mixes were comparable. Mix 4 extended the time to cracking by 23 % and Mixes 3, 5 and 6 slightly decreased in cracking time

by 10 %, 13 %, and 15 % respectively. This may be due to the relatively short time that the inhibitor had to penetrate the samples (only 24 days) and the severity of the accelerated test. On the other hand, Mix 2, which incorporated cinnamaldehyde encapsulated in LWA, required 52.1 ± 15.9 d for the sample to crack. This may be due to creation of a protective cinnamaldehyde film on the steel rebar or, as the agent diffuses into the pore solution, some change the solution physicochemical properties that slows the diffusion of chloride ions occurs [23]. The exact details of the protective mechanism require further research.

The initial electrical resistivity values of each mix, except Mix 2, begin at around 5 kΩ•cm (Fig. 8). A similar trend was observed for each mix: electrical resistivity increased with time until a crack initiated. A similar trend was observed by Polder and Peelen, where it was concluded that the electrical resistivity of concrete influences the likelihood of corrosion and the rate of corrosion [24]. The use of water-LWA and penetrating corrosion inhibitor-LWA did not

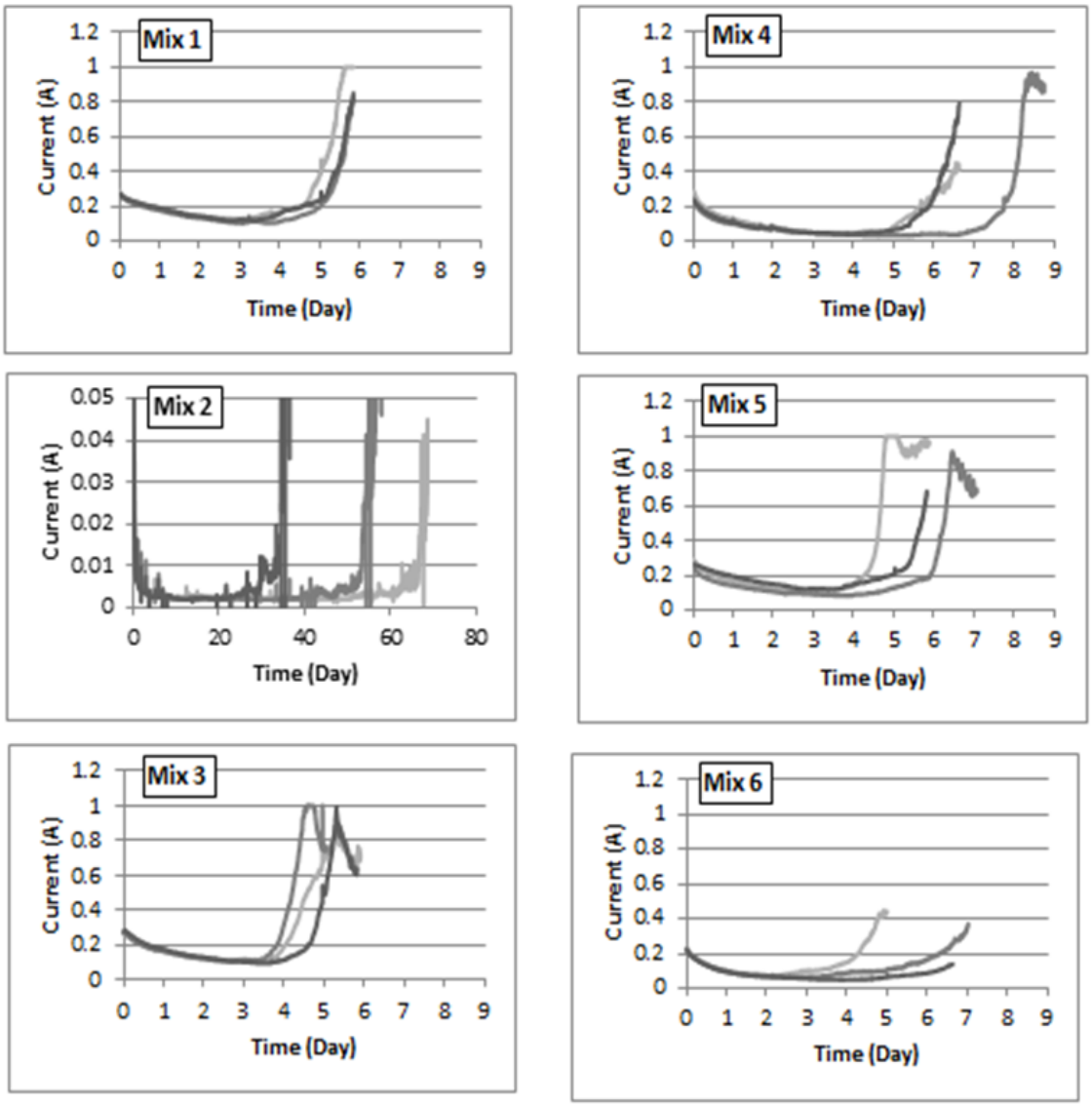

Figure 7: Accelerated corrosion test results. N.b.: for Mix 2, the x-axis is larger and the y-axis is smaller.

significantly impact the resistivity; however, the use of surface applied penetrating corrosion inhibitor did cause some variation by creating a slight overall increase in resistivity. The resistivity of Mix 2 was significantly increased, due to the cinnamaldehyde being an organic material, as discussed above. As the test progressed, low standard deviations were initially observed for the resistivity measurements. Over time, the deviations increased due to the readings being taken on four sides of each sample. Resistivity is drastically lowered in the area of a saturated crack, causing the increase in deviation.

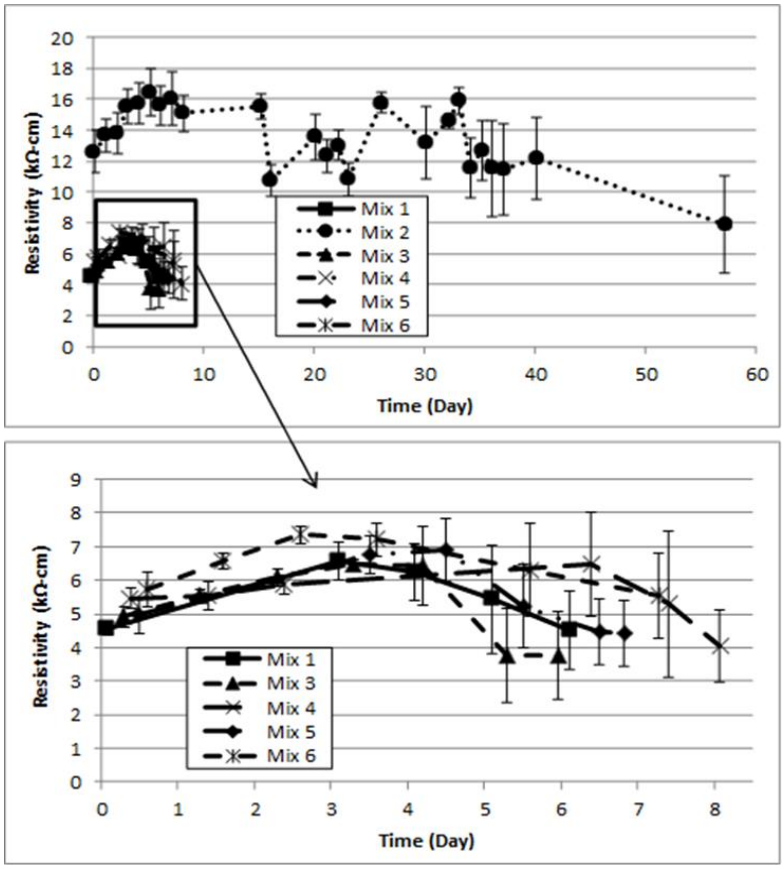

Figure 8: Electrical resistivity of lollipop samples as determined by Wenner probe. The electrical resistivity of Mixes 1, 3, 4, and 5 are enlarged in the lower plot.

After impressing a constant 30 V on the lollipop samples during the ACT, the mass loss of the reinforcing steel was calculated and compared with cracking time (Fig. 9). The greatest steel mass loss was observed in the water-LWA of Mixes 3 and 5 (36.5 ± 2.8 g and 37.3 ± 9.8 g, respectively). Mixes 1, 2, and 4 had similar results, with losses of 31.5 ± 5.3 g, 21.8 ± 13.2 g, 23.4 ± 5 g, respectively. Mix 6 experienced the least amount of steel mass loss of 17.9 ± 2.9 g. This indicates that cinnamaldehyde-LWA and penetrating corrosion inhibitor-LWA did not significantly impact the mass loss of the reinforcing steel during corrosion. Surface application of the penetrating corrosion inhibitor seemed to protect the rebar from losing mass, while water-LWA permitted a large mass loss before failure. Elmoaty conducted a similar test on lollipop samples [25], determining that the high voltage (30 V) used in the ACT may affect the results. If a lower voltage were used over a longer time period, more accurate results might be produced.

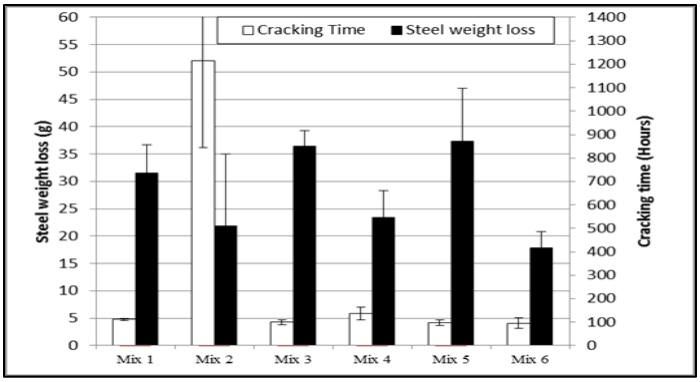

Figure 9: Mass loss of reinforcing steel and corresponding cracking time.

Phase II:

The second part of this study involved a further investigation of cinnamaldehyde-LWA incorporation into a cementitious mix. Studies that were carried out included: compressive strength, isothermal calorimetry, sorptivity, diffusion, and rebar pullout. (Note: compressive strength tests were re-done since a slightly modified mix design was used).

Materials and Methods

Three mortar mixes were produced and tested. The first mix, Mix 1, served as the control and was composed of local sand, ASTM C150 Type I/II cement, and water. The two other mixes (Mix 2 and Mix 3) were experimental and consisted of the same components as Mix 1, but included a partial replacement of the sand with presoaked LWA. Mix 2 contained water-LWA and Mix 3 contained a cinnamaldehyde-LWA. Each mix had a water:cement ratio of 0.4 (not including the water stored within the LWA) and a 55 % volume fraction of aggregate. The complete components for each mix are shown in Table 3. LWA was soaked in water for at least 24 h in a sealed container. After 24 h, the pre-wet LWA was then incorporated into Mix 2 in a saturated surface dry (SSD) state. The same method was used for encapsulating cinnamaldehyde into the LWA for Mix 3.

The LWA was commercially available expanded shale (Northeast Solite Corporation) with an absorption capacity of 17.5 % by mass (provided by manufacturer). Mixes that included LWA involved a partial replacement of the local sand with LWA on a volumetric basis in order to retain the same particle size distribution as the sand. The amount of LWA needed for the mixes was calculated by [10]:

$$M_{LWA} = \frac{C_f \times CS \times \alpha_{max}}{S \times \Phi_{LWA}} \quad (2)$$

where M_{LWA} is the mass of LWA; C_f is the cement factor; CS is the chemical shrinkage of the binder (determined using ASTM C1608 - Fig. 10); α_{max} is maximum degree expected for the

Table 3: Mix designs for Phase II

		Mix 1		Mix 2		Mix 3	
		Volume (cm^3)	Mass (g)	Volume (cm^3)	Mass (g)	Volume (cm^3)	Mass (g)
Sand (total)		1375.0	3588.8	1046.7	2731.9	1046.7	2731.9
LWA (total)		N/A	N/A	328.3	492.5	328.3	492.5
#8	Sand	412.5	1076.6	314.0	819.6	314.0	819.6
	LWA	N/A	N/A	98.5	147.7	98.5	147.7
#16	Sand	343.8	897.2	261.7	683.0	261.7	683.0
	LWA	N/A	N/A	82.1	123.1	82.1	123.1
#30	Sand	275.0	717.8	209.3	546.4	209.3	546.4
	LWA	N/A	N/A	65.7	98.5	65.7	98.5
#50	Sand	206.3	538.3	157.0	409.8	157.0	409.8
	LWA	N/A	N/A	49.2	73.9	49.2	73.9
#100	Sand	137.5	358.9	104.7	273.2	104.7	273.2
	LWA	N/A	N/A	32.8	49.2	32.8	49.2
Mixing water		585.4	585.4	585.4	585.4	585.4	585.4
Cement		464.6	1463.5	464.6	1463.5	464.6	1463.5
Internal water		N/A	N/A	86.2	86.2	N/A	N/A
CA		N/A	N/A	N/A	N/A	86.2	90.5

reaction of the binder; S is the saturation level; and Φ_{LWA} is the sorption capacity of the LWA (Table 4).

The compressive strength of all mixes was determined in accordance with ASTM C109. Once mixed, the mortar (at least three samples per mix) was immediately placed and tamped into 2 in. (50 mm) cube molds, sealed in a plastic bag, and stored in a fog room. Samples were demolded after 24 h and placed back into the fog room to cure, and tested at ages of 3, 7, 28, and 91 d.

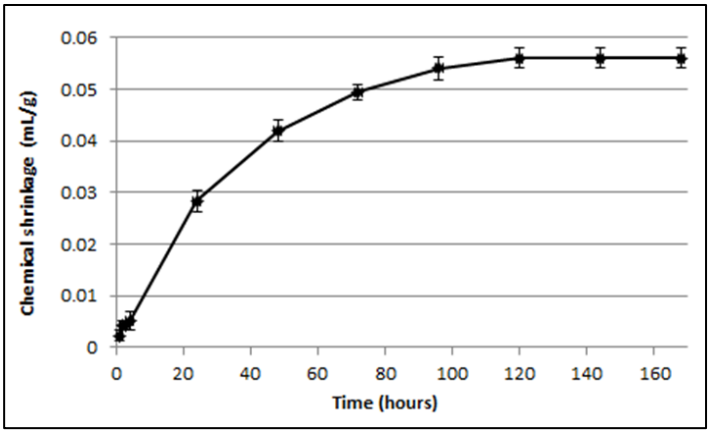

Figure 10: Chemical shrinkage

Isothermal calorimetry was used to assess the hydration kinetics of the mortars. The heat flow of the mortars was evaluated during the initial 24 h of hydration. Two samples of each mix were investigated. Once mortars were mixed, the appropriate amount was immediately placed in an ampoule and sealed closed. The calorimeter was set to be normalized to the grams of cement in the mix.

Sorptivity tests were conducted following ATSM C1585. Mortar was placed into 4 x 2 in. (100 x 50 mm) cylinders, stored in a fog room, demolded after 24 h and placed back in the fog room to cure for 28 d. On day 28, the samples were removed from the fog room and placed in an oven at 105 °C to dry for 24 h. Once removed from the oven and cooled, the circumference of the cylinder was sealed using duct tape in order ensure unidirectional sorption. The samples were then placed on supports at the bottom of an enclosed plastic tank. Water was filled into the tank such that it was 0.08 ± 0.04 in. (2 ± 1 mm) above the bottom of the sample; the water level was maintained at that level throughout the experiment. Three samples per mix were investigated. Absorption, I, was calculated by:

$$I = \frac{m_t}{a \times d} \tag{3}$$

where I is the absorption, m_t is the change in mass at time t, a is the exposed area of the sample (mm^2), and d is the density of water (g/mm^3).

Both the initial and secondary rate of water are identified as the slope of the line to the absorption plotted against the square root of time. To characterize initial sorptivity, the masses of the sample were taken at 60 s, 5 min, 10 min, 20 min, 30 min, 60 min, and every hour for the following 6 h. The slope of the plot is the initial rate of absorption. The secondary rate of absorption is found in the same manner as the initial rate but at later ages. Masses were recorded once every ~ 24 h for a total of 7 d.

Table 4: Values used to calculate M_{LWA}

Variable	Value
C_f	585 kg/m^3
CS	0.056 mL/g
α_{max}	1
S	0.95
Φ_{LWA}	0.175

The diffusion of NaCl through these mortars was examined. Mortar was placed in 4 x 8 in. (100 x 200 mm) cylinder molds. A total of three samples were investigated per mix. After 28 d curing, the cylinders were each immersed in a 5 % (by mass) NaCl solution stored in a sealed plastic tank for 3 months. The samples were removed from the solution, split lengthwise, and sprayed with silver nitrate ($AgNO_3$) [26, 27]. The silver nitrate changes the color of the mortar such that where there is a concentration of chloride ions, the mortar is lighter in color (normally around the top, bottom, and sides). A computing program provided by the NIH (ImageJ) detected the difference in color through a binarization of an image of the sample. From this, the area that the chloride traveled could be calculated.

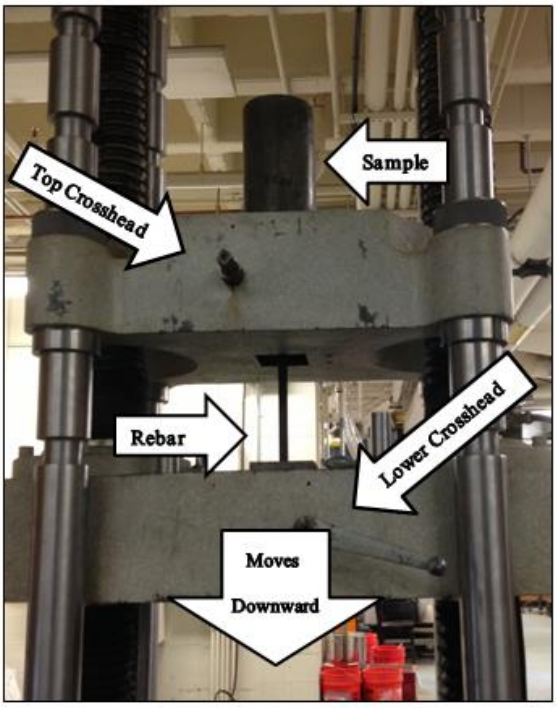

Figure 11: Rebar pullout setup

Moreover, to identify if the experimental mixes, Mix 2 and 3, interfered with the bond strength between mortar and rebar, rebar pullout test were carried out [28]. Samples were prepared by placing mortar into 6 x 12 in. (152.4 x 304.8 mm) cylinders and embedding a ¾ in. (19.1 mm) wire-brushed rebar of 3 ft. (91.4 cm) length in the center. To ensure perpendicular alignment a jig was made to hold the rebar in place. Once cured for 28 d, the samples (three for each mix type) were placed on the top crosshead of a Tinius Olsen Loading machine where the rebar ran through the lower crosshead and was secured by jaws (Fig.11). A shim was put in between the top of the tensile frame and the cylinder to reduce the effects of eccentricity. A displacement rate of 0.1 in/min was used.

Results and Discussion

Mixes containing presoaked LWA resulted in lower compressive strengths (Fig. 12). Mix 2 – water soaked LWA- resulted in reduced strengths when compared to the control by 4 % at 3 d and 7 d; 8 % at 28 d; and 7 % at 91 d. This decrease in strength is due to the weak nature (due to the existing pores) of the LWA as discussed above [19]. However, when using LWA to encapsulate cinnamaldehyde (Mix 3) larger reductions in strength were observed. Compressive strength decreased by 31% at 3 d, 33 % at 7 d, 40% at 28 d, and 41 % at 91 d. This indicates that the surplus of liquid is remaining on the surface of the LWA, and entering the mix or LWA is pre-releasing the cinnamaldehyde and interfering with the

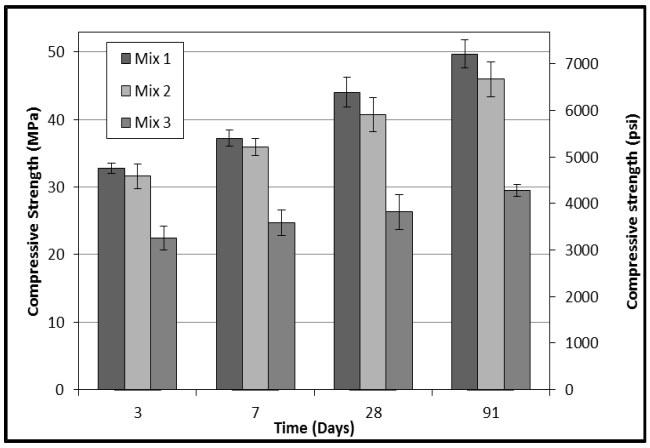

Figure 12: Compressive strength of mortars at ages 3, 7, 28, and 91 d.

hydration reactions as previously discussed.

Hydration is an exothermic reaction and the hydration kinetics of the mixes was observed (Fig. 13). Mix 2 displayed a slight acceleration to the control (Mix 1). This has been previously observed and is due to the additional hydration [29]. However, Mix 3 was shown to have a severe retardation with a 14 % reduction of heat flow compared to the control. Also, Mix 3 a leftward shift in the in the graph further indicating severe interferences.

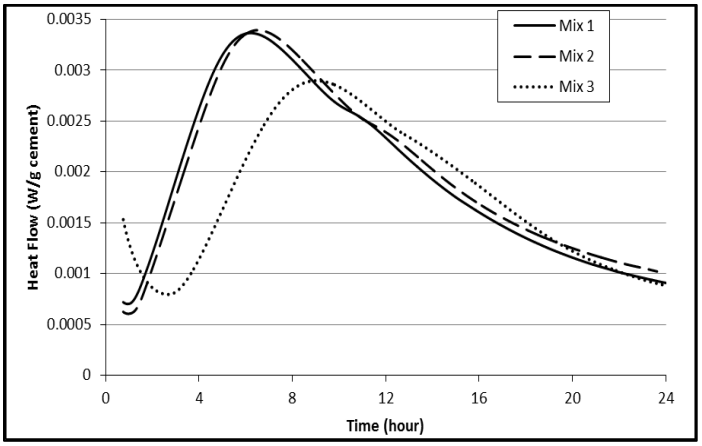

Figure 13: Isothermal calorimetry

The results of the initial rate of absorption follow a linear relationship with a correlation coefficient of 0.98 or greater (Fig. 14). The sorptivity coefficient of Mix 2 was slightly larger when compared to the control within the first 6 h (Table 5). Since sorptivity relates to the ability of the pore structure to absorb liquid by capillary forces, this may explain the reason for Mix 2 to have the greatest initial sorptivity[30]. The "open" pores of the LWA may be reason to this since the LWA releases its stored water and thus leaves empty pores which can absorb a larger amount of water. However, the addition of cinnamaldehyde (Mix 3) led to a lower initial sorptivity coefficient compared to the control. This may be due to cinnamaldehyde filling the pores through the initial phases.

However, the secondary rate of water absorption for Mix 1 and Mix 2 did not follow a correlation coefficient of 0.98 or greater (coefficients of 0.945 and 0.934 were calculated for Mix 1 and Mix 2 respectively) (Fig. 15); this has previously occurred in the literature [31]. Although a direct linear relationship was not found, some indications from the regression equations can be noted (Table 6). The during 1 d through 7 d, the sorptivity coefficients of Mix 1 and Mix 2 decreased from the initial coefficients. These follow the traditional trend of sorptivity decreasing with an increase of age [30]. However, the secondary rate of water absorption for Mix 3 increased slightly. This may be due to the LWA as mentioned above.

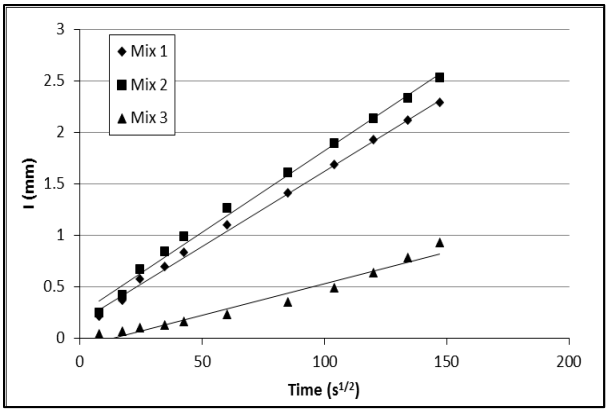

Figure 14: Initial rate of water absorption

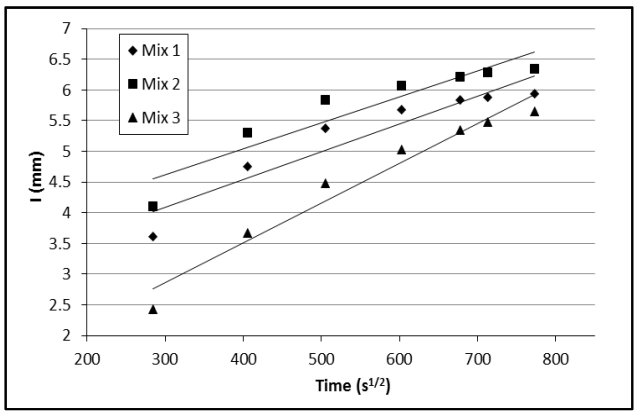

Figure 15: Secondary rate of water absorption

Table 5: Regression equations of initial rate of water absorption

Sample	Regression equation	Correlation coefficient	Sorptivity coefficient ($mm/s^{1/2}$)
Mix 1	y = 0.0146x + 0.163	0.998	0.0146
Mix 2	y = 0.0159x + 0.240	0.997	0.0159
Mix 3	y = 0.0061x - 0.082	0.980	0.0061

Table 6: Regression equations of initial rate of water absorption

Sample	Regression equation	Correlation coefficient	Sorptivity coefficient ($mm/s^{1/2}$)
Mix 1	y = 0.0045x + 2.7285	0.945	0.0045
Mix 2	y = 0.0042x + 3.3381	0.934	0.0042
Mix 3	y = 0.0065x + 0.9166	0.980	0.0065

Additionally, the mixes were investigated for diffusion of NaCl through the mortars (Fig. 16). The area, in percentage of the sample, of chloride that penetrated Mix 2 was 23 % less when compared to the control (Mix 1). This may be due to the LWA creating a denser microstructure due to the additional hydration of the additional water [20]. The diffusion of NaCl through Mix 3 was 17 % less than the control. This can be due to the cinnamaldehyde filling the pores within the cementitious matrix resulting in a more dense microstructure as well (Fig. 17).

The bond stresses of the mixes were determined. Results of the rebar pullout show that Mix 2 has the greatest bond stress (Fig. 18). The failure pattern of Mix 2 also reveals that gradual failure (with plateaus-like behavior) prolonging the time to failure and thus producing the greatest bond

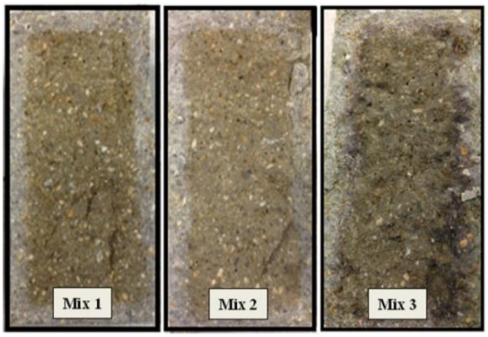

Figure 16: Samples of cylinders split lengthwise and sprayed with silver nitrate after exposed to NaCl solution bath for 3 m.

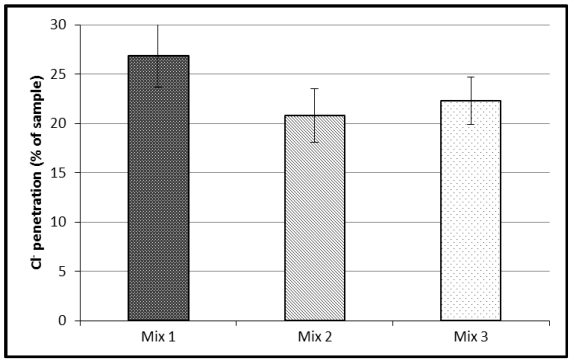

Figure 17: Total percent of the area that chloride penetrated the samples.

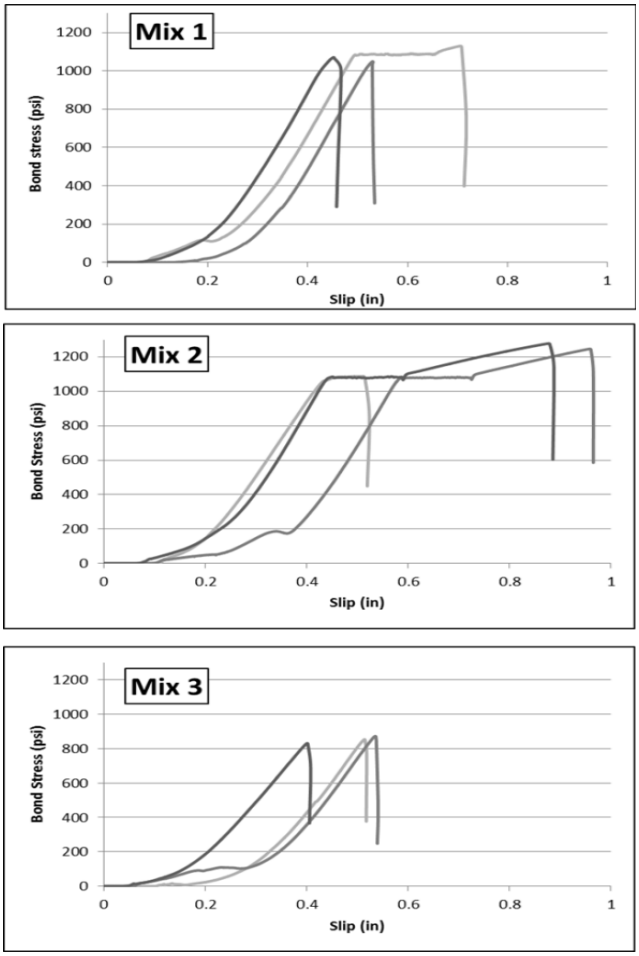

Figure 18: Rebar pullout results plotted as bond stress over slip

stress. This may be due to the denser microstructure of the mix. However, Mix 3 yields the lowest bond stress with a sharp failure mode (as opposed to the plateaus observed in Mix 2). The coating of cinnamaldehyde onto the rebar may be causing a larger slip between the interface of the rebar and mortar. Further studies and analyses may be needed to fully determine the reasons for such failures.

Conclusions

A study on the use of LWA encapsulating liquids as an incorporation method for corrosion mitigation has been carried out. The addition of mitigation agents via LWA caused the time of set to increase, lower compressive strengths, and lower peak internal temperatures, indicating interferences with the hydration of the cement. Detection of autogenous expansion signifies the diffusion of the internal agents into the cementitious matrix. The sorptivity of water and diffusion of NaCl through its mix was decreased suggesting a denser microstructure. This technology, however, is still promising due to the significantly prolonged corrosion resistance observed by the inclusion of the cinnamaldehyde. Future research should include a study on the substantial increase in corrosion life when using the cinnamaldehyde-LWA. Additional research on including LWA as a transport mechanism for corrosion mitigation agents without affecting the hydration should be studied.

Acknowledgements

The PIs would like to thank the American Concrete Institute (ACI) for funding this experimental program.

References

1. Koch, G.H., et al., *Corrosion cost and preventive strategies in the United States*. 2002.
2. Emmons, P.H.a.D.J.S., *The State of the Concrete Repair Industry, and a Vision for its Future*. Concrete Repair Bulletin, 2006: p. 7-14.
3. Böhni, H., *Corrosion In Reinforced Concrete Structures*. 2005: Woodhead pub.
4. Cabrera, J.G., *Deterioration of concrete due to reinforcement steel corrosion.* Cement and Concrete Composites, 1996. **18**(1): p. 47-59.
5. Slater, J.E., *Corrosion of Metals in Association With Concrete: A Manual*. 1983: American Society for Testing and Materials.
6. Lindquist, W.D., et al., *Effect of cracking on chloride content in concrete bridge decks.* ACI Materials Journal, 2006. **103**(6): p. 467.
7. Şahmaran, M. and V.C. Li, *De-icing salt scaling resistance of mechanically loaded engineered cementitious composites.* Cement and Concrete Research, 2007. **37**(7): p. 1035-1046.
8. Li, F., Y. Yuan, and C.-Q. Li, *Corrosion propagation of prestressing steel strands in concrete subject to chloride attack*. Construction and Building Materials, 2011. **25**(10): p. 3878-3885.
9. Jafferji, H.K., Gregory T.; Schiffman, Jessica D.; Sakulich, Aaron R., *Preliminary Investigations of Essential Oils as Corrosion Inhibitors in Steel Reinforced Cementitious Systems.* Proceeding of the Thrity-Fifth Conference on Cement Microscopy, USA, 2013: p. 40-48.
10. Bentz, D.P. and W.J. Weiss, *Internal curing: A 2010 state-of-the-art review*. 2011: US Department of Commerce, National Institute of Standards and Technology.
11. Güneyisi, E., T. Özturan, and M. Gesoğlu, *A study on reinforcement corrosion and related properties of plain and blended cement concretes under different curing conditions.* Cement and Concrete Composites, 2005. **27**(4): p. 449-461.
12. Güneyisi, E., et al., *Corrosion behavior of reinforcing steel embedded in chloride contaminated concretes with and without metakaolin.* Composites Part B: Engineering, 2013. **45**(1): p. 1288-1295.
13. Ahmad, S., *Techniques for inducing accelerated corrosion of steel in concrete.* Arabian Journal for Science and Engineering, 2009. **34**(2): p. 95.
14. Detwiler, R.J., K.O. Kjellsen, and O.E. Gjorv, *Resistance to chloride intrusion of concrete cured at different temperatures.* ACI Materials Journal, 1991. **88**(1).
15. Gowers, K. and S. Millard, Measurement of Concrete Resistivity for Assessment of Corrosion Severity of Steel using Wenner Technique. ACI Materials Journal, 1999. **96**(5).
16. Shaker, F., A. El-Dieb, and M. Reda, *Durability of styrene-butadiene latex modified concrete.* Cement and concrete Research, 1997. **27**(5): p. 711-720.
17. Okba, S., A. El-Dieb, and M. Reda, *Evaluation of the corrosion resistance of latex modified concrete (LMC).* Cement and concrete research, 1997. **27**(6): p. 861-868.
18. Al-Zahrani, M., et al., *Effect of waterproofing coatings on steel reinforcement corrosion and physical properties of concrete.* Cement and Concrete Composites, 2002. **24**(1): p. 127-137.
19. Bentz, D.P., *Internal curing of high-performance blended cement mortars.* ACI Materials Journal, 2007. **104**(4): p. 408.
20. Bentz, D.P., K.A. Snyder, and M.A. Peltz, *Doubling the service life of concrete structures. II: Performance of nanoscale viscosity modifiers in mortars.* Cement and

Concrete Composites, 2010. **32**(3): p. 187-193.
21. Bentur, A., S.-i. Igarashi, and K. Kovler, *Prevention of autogenous shrinkage in high-strength concrete by internal curing using wet lightweight aggregates.* Cement and concrete research, 2001. **31**(11): p. 1587-1591.
22. Labes, M.M., R. Sehr, and M. Bose, *Organic Semiconductors. II. The Electrical Resistivity of Organic Molecular Complexes.* The Journal of Chemical Physics, 2004. **33**(3): p. 868-872.
23. Cusson, D., Z. Lounis, and L. Daigle, *Benefits of internal curing on service life and life-cycle cost of high-performance concrete bridge decks–A case study.* Cement and Concrete Composites, 2010. **32**(5): p. 339-350.
24. Polder, R.B. and W.H. Peelen, *Characterisation of chloride transport and reinforcement corrosion in concrete under cyclic wetting and drying by electrical resistivity.* Cement and Concrete Composites, 2002. **24**(5): p. 427-435.
25. Elmoaty, A. and A.E. Mohamed, *Mechanical properties and corrosion resistance of concrete modified with granite dust.* Construction and Building Materials, 2013. **47**: p. 743-752.
26. Baroghel-Bouny, V., et al., *AgNO3 spray tests: advantages, weaknesses, and various applications to quantify chloride ingress into concrete. Part 1: Non-steady-state diffusion tests and exposure to natural conditions.* Materials and structures, 2007. **40**(8): p. 759-781.
27. Baroghel-Bouny, V., et al., *AgNO3 spray tests: advantages, weaknesses, and various applications to quantify chloride ingress into concrete. Part 2: Non-steady-state migration tests and chloride diffusion coefficients.* Materials and Structures, 2007. **40**(8): p. 783-799.
28. Chen, G., et al., *Coated Steel Rebar for Enhanced Concrete-Steel Bond Strength and Corrosion Resistance*. 2010.
29. Bentz, D.P., *Influence of internal curing using lightweight aggregates on interfacial transition zone percolation and chloride ingress in mortars.* Cement and concrete composites, 2009. **31**(5): p. 285-289.
30. Lo, T.Y., et al., *The effects of air content on permeability of lightweight concrete.* Cement and concrete research, 2006. **36**(10): p. 1874-1878.
31. Ghafari, E., et al., *The effect of nanosilica addition on flowability, strength and transport properties of ultra high performance concrete.* Materials & Design, 2014. **59**: p. 1-9.